Title

Endorectal MRI and MR spectroscopic imaging of prostate cancer: Developing selection criteria for MR-guided focal therapy

Journal

Journal of Magnetic Resonance Imaging, 39(3)

ISSN

1053-1807

Authors

Chang, Stephanie T

Westphalen, Antonio C

Jha, Priyanka

et al.

Publication Date

2014-03-01

DOI

10.1002/jmri.24187

Peer reviewed

Published in final edited form as:
J Magn Reson Imaging. 2014 March ; 39(3): 519–525. doi:10.1002/jmri.24187.

Endorectal MR imaging and MR spectroscopic imaging of prostate cancer: Developing selection criteria for MR-guided focal therapy

Stephanie T. Chang, MD[1], **Antonio C. Westphalen, MD**[1], **Priyanka Jha, MB BS**[1], **Adam J. Jung, MD PhD**[1], **Peter R. Carroll, MD MPH**[2,3], **John Kurhanewicz, PhD**[1,3], and **Fergus V. Coakley, MD**[1,2,3]

[1]Department of Radiology and Biomedical Imaging, University of California, San Francisco

[2]Department of Urology, University of California, San Francisco

[3]University of California, San Francisco Helen Diller Family Comprehensive Cancer Center

Abstract

Purpose—To investigate criteria that can identify dominant treatable prostate cancer foci with high certainty at endorectal MRI and MR spectroscopic imaging, and thus facilitate selection of patients who are radiological candidates for MR-guided focal therapy.

Materials and methods—We retrospectively identified 88 patients with biopsy-proven prostate cancer who underwent endorectal MRI and MR spectroscopic imaging prior to radical prostatectomy with creation of histopathological tumor maps. Two independent readers noted the largest tumor foci at MRI, if visible, and the volume of concordant abnormal tissue at MR spectroscopic imaging, if present. A logistic random intercept model was used to determine the association between clinical and MR findings and correct identification of treatable (over 0.5 cm^3) dominant intraprostatic tumor foci.

Results—Readers 1 and 2 identified dominant tumor foci in 50 (57%) and 58 (65%) of 88 patients; 42 (84%) and 48 (83%) of these were dominant treatable lesions at histopathology, respectively. Within the statistical model, the volume of concordant spectroscopic abnormality was the only factor that predicted correct identification of a dominant treatable lesion on T2-weighted images (odds ratio = 1.75; 95% confidence interval = 1.08 to 2.82; p-value = 0.02). In particular, all visible lesions on T2-weighted imaging associated with at least 0.54 cm^3 of concordant spectroscopic abnormality were correctly identified dominant treatable tumor foci.

Conclusion—Patients with dominant intraprostatic tumor foci seen on T2-weighted MRI and associated with at least 0.54 cm^3 of concordant MR spectroscopic imaging abnormality may be radiological candidates for MR-guided focal therapy.

Keywords

Prostate cancer; Focal therapy; High intensity focused ultrasound; MR imaging; MR spectroscopic imaging

Corresponding Author Fergus Coakley MD 505 Parnassus Avenue, M-372, Box 0628 San Francisco, CA, 94143 Telephone: (415) 353-1821 / Fax: (415) 476-0616 fergus.coakley@radiology.ucsf.edu.

Introduction

Since the first report of successful prostate cancer treatment by unilateral nerve-sparing cryosurgery in 2002 (1), the concept of focal therapy for prostate cancer has generated considerable discussion and controversy. Proponents argue that focal ablative therapies provide a middle ground between the definitive but morbid options of radical prostatectomy or radiation and the minimalist approach of active surveillance (2-5)(1-4). Despite many conceptual advantages, there are two major hurdles to implementing a focal therapy program for prostate cancer. First, the correct subset of patients must be identified so that patients with indolent or subclinical disease may be offered the management option of active surveillance while patients with aggressive disease receive appropriately radical treatment. This is a biological question, and accurate risk stratification of patients with prostate cancer is a non-trivial challenge (6). Second, assuming appropriate candidates can be clinically selected, the cancer must be correctly identified and precisely ablated during the focal therapy (3). This is primarily a radiological problem. The high rate of complications reported after current focal therapies for prostate cancer such as ultrasound-guided focused ultrasound or cryosurgery likely reflects imprecise treatment targeting and monitoring, resulting in unintended injuries to nearby structures including the rectum and neurovascular bundles (7, 8). The recent emergence of endorectal MR-guided focused ultrasound surgery as a method of prostate cancer ablation provides a novel and exciting approach to focal therapy that promises precisely targeted tissue necrosis with real-time monitoring by MR thermometry (9)(5). Some human subjects have already undergone technically successful endorectal MR guided focused ultrasound surgery of prostate cancer outside the United States (*Kobi Vortman PhD, personal communication)*. In this country, Food and Drug Administration approval will be required before interested institutions can provide this investigational technology to American men. MR-guided focal therapy can also be performed using MR-guided laser ablation (10). While saturation biopsy without imaging could theoretically be used to determine the target of such MR-guided focal ablative therapies (11), MR-guided focal therapy seems best suited to patients with a visible dominant tumor at MRI, so that treatment is delivered to a tumor depicted by the same modality that is being used to guide therapy. This avoids the potential inaccuracies in "blindly" treating a designated portion of the prostate based purely on positive biopsies. Previous studies have demonstrated that endorectal MRI and MR spectroscopic imaging may improve tumor localization, staging, and volume estimation to allow non-invasive identification of prostate cancer (12-14), but it is unknown whether and how these techniques can be used to select patients eligible for focal therapy by detecting the dominant intraprostatic tumor focus. Ideally, MR targets would be identified with high sensitivity and specificity. At a minimum, it seems reasonable to require that dominant tumor sites should be identified with high certainty when selecting patients for MR guided focused ultrasound surgery. The rationale for this statement is that focally treating a false positive tumor with an emerging technology rather than conventional treatment is ethically problematic and clinically risky since the true site of dominant disease would presumably be untreated. In addition, not offering investigational therapy to patients with uncertain dominant tumor foci seems ethically justifiable, since they are still candidates for all orthodox managements and have not been denied any standard treatment. Accordingly, we undertook this study to investigate criteria that can identify dominant treatable prostate cancer foci with high certainty at endorectal MRI and MR spectroscopic imaging, and thus facilitate selection of patients who are radiological candidates for MR-guided focal therapy.

Materials and methods

Subjects

This single institution retrospective study was approved by our Committee on Human Research with a waiver of informed consent and was compliant with the Health Insurance Portability and Accountability Act. We identified all patients who met the following inclusion criteria:

- Endorectal MR and MR spectroscopic imaging of the prostate performed for biopsy-proven prostate cancer between 2000 and 2006.
- Radical prostatectomy performed with creation of detailed tumor maps from step-section histopathological evaluation of the specimen.
- No interval prostate cancer treatment administered between MRI and prostatectomy.

We identified 101 eligible patients, but 13 patients were excluded because the histopathological records could not be found (n = 7) or because the MR images were not retrievable (n = 6). Subsets of the study population have been included in previous studies (14-17). The lead investigator (--) reviewed all available medical records to determine pertinent patient demographic and clinical parameters. The final study population of 88 men had a mean age of 59 years (range, 45 to 75). The median biopsy Gleason score was 6 (range, 5 to 9). The mean serum prostate-specific antigen level at diagnosis was 9.2 ng/mL (range, 1.7 to 64.1). Clinical stage on digital rectal examination performed by a urologist was T1 in 15 patients, T2 in 34 patients, and undocumented in 35 patients. The mean interval between endorectal MRI and MR spectroscopic imaging and radical prostatectomy was 79 days (range, 2 to 555, with an interval exceeding 6 months in only 9 patients).

MR technique

MRI was performed on a 1.5T whole-body MR scanner (Signa; GE Medical Systems, Milwaukee, WI). The patients were imaged in the supine position using a body coil for signal excitation and a pelvic phased-array coil (GE Medical Systems) combined with a balloon-covered expandable endorectal coil (Medrad, Pittsburgh, PA) for signal reception. Axial spin-echo T1-weighted images were obtained from the aortic bifurcation to the symphysis pubis using the following parameters: repetition time msec/echo time of 700/8 msec, 5-mm section thickness, 1-mm intersection gap, 24 cm field of view, 256 × 192 matrix, transverse frequency direction, and one signal excitation acquired. Thin-section high-spatial-resolution axial and coronal T2-weighted fast spin-echo MR images of the prostate and seminal vesicles were then obtained using the following parameters: repetition time msec/effective echo time of 6000/96 msec, echo train length of 16, 3-mm section thickness, no intersection gap, 14 cm field of view, 256 × 192 matrix, and three signal excitations acquired. All MR images were routinely post-processed to compensate for the reception profile of the endorectal and pelvic phased-array coils. After review of the axial T2-weighted images, an MR spectroscopic imaging volume of 110 × 55 × 55 mm was selected to maximize coverage of the prostate, while minimizing the inclusion of periprostatic fat and rectal air. Three-dimensional MR spectroscopic imaging data were acquired using a water and lipid suppressed double-spin echo point-resolved spectroscopy sequence technique. Spectral-spatial pulses optimized for the quantitative detection of choline, creatine, polyamines, and citrate were used for the two 180° excitations [18, 19]. Outer voxel saturation pulses were employed to further sharpen volume selection to the shape of the prostate and eliminate susceptibility artifact from periprostatic fat and rectal air (20). Data sets were acquired with a repetition time/echo time of 1000/130 msec, 16 × 8 × 8 phase-encoded spectral array, and a 17-minute acquisition time. This spectral array resulted

in cubic voxels measuring 6.875 mm in each dimension and a voxel size of 0.32cm^3. The spectroscopic imaging data were zero-filled from 8 to 16 in both the anteroposterior and craniocaudal directions to increase the likelihood of optimal alignment between spectroscopic voxels and the prostate, and yielding a nominal spectral resolution of 0.09 cm^3. Three-dimensional MR spectroscopic imaging data were processed off-line on an UltraSparc workstation (Sun Microsystems, Mountain View, CA) utilizing in-house software. Integrated peak area values for choline, creatine, and citrate and peak area ratios for choline to creatine and choline plus creatine to citrate were automatically calculated for each voxel. MR spectroscopic imaging data (spectra and associated metabolic ratios) were overlaid on the corresponding axial T2-weighted images, and these processed images were sent to our PACS system to become an integral part of the archived MR study.

Image Interpretation

Two readers (ACW and AJJ) with 12 and 4 years of experience, respectively, in the interpretation of endorectal MRI and MR spectroscopic imaging of the prostate independently reviewed all MR and MR spectroscopic images on a picture archiving and communication system workstation (Impax; Agfa, Mortsel, Belgium). Readers knew that patients had biopsy-proven prostate cancer, but were unaware of any other clinical data or histopathological results. Readers recorded the location and bi-dimensional size in millimeters of the dominant tumor focus (if present) on a standardized prostate map. The dominant tumor focus was defined as the largest focus of ovoid mass-like or crescentic subcapsular T2 signal reduction that was considered to be malignant based on the expert judgment of the readers and based on the totality of MR findings. This definition did not require associated abnormal spectroscopic findings to be present in the dominant tumor focus, but such findings could influence the designation of dominant tumor focus. Readers also recorded the number of associated voxels demonstrating suspicious or unequivocal malignant metabolism on MR spectroscopic imaging, defined as the presence of a choline peak of similar or greater size than the citrate peak (21). MR spectroscopic imaging tumor volume was calculated by multiplying the number of such voxels by the nominal voxel size after zero-filling (0.09 cm^3). For example, if 10 voxels were considered to display unequivocal malignant metabolism, the calculated MRSI tumor size was 0.9 cm^3.

Histopathological review

Specimens removed at radical prostatectomy were marked with ink and fixed overnight in 10% buffered formalin. Transverse step sections were obtained at 3 to 4 mm intervals in a plane perpendicular to the prostatic urethra. Paraffin sections were cut at 3 microns and stained with hematoxylin and eosin for preparation of slides. An attending pathologist reviewed the slides and recorded the size, location, and Gleason score of all cancer foci on a standardized map of the prostate. Histopathological tumor volumes were estimated using the formula for tumor volume of $(4/3)\pi\ (D/2)^3$, where D is the average of the maximum and minimum axial diameters of the histopathological tumor (22).

Statistical analysis

The major endpoint of this study was the correct identification of dominant treatable foci of prostate cancer. While the clinical characteristics of what constitutes a treatable focus for local ablation remain in flux (6, 23), there is general acceptance in the urological community that a prostate cancer focus of over 0.5 cm^3 in volume identifies clinically relevant disease (24). As such, we considered a treatable dominant prostate cancer focus to be present in a patient if the largest tumor focus had a histopathological volume of over 0.5 cm^3. The principal investigator (--) compared the histopathological tumor maps with the standardized tumor maps generated by the readers, to determine which visualized tumors were true positive and false positive dominant foci. Specifically, a dominant focus of prostate cancer

was considered to be correctly identified if the dominant focus identified by the readers corresponded to the dominant focus on the histopathological tumor map. Anatomic landmarks and tumor laterality, size, and location were used to assist this co-registration and determination by the principal investigator (while co-registration and accurate distinction of true and false positives can be problematic for smaller lesions, our experience during this study confined to the identification of dominant foci was that this determination was generally straightforward). A logistic random intercept model was used to determine the association between clinical variables and MR findings and correct identification of treatable dominant prostate cancer foci (i.e., those dominant foci with a histopathological volume of over 0.5 cm^3) while adjusting for correlation between readers. This particular statistical model was used because it accounts for the effect of repeated measures (in our study, the observations by two different readers on the same imaging dataset) and quantifies the extent to which inter-reader variation is random as against reflecting real interpretative differences. The latter is expressed as the intra-class correlation. We conducted both forward and backward stepwise processes to select the variables that would be included in the final model (p-value criteria, 0.05 for entry and 0.1 for staying). These are rigorous statistical methods in which the choice of predictor variables included in the model is done automatically. In the forward selection the process starts without any variables in the model, and continuous by testing the variables one by one, including only statistically significant ones. In the backward selection process, the model starts with all variables, which are also individually tested and eliminated if not statistically significant. Because the methods are not necessarily complementary or equivalent, we opted for using both methods and then compare the models obtained. We used likelihood ratio and Wald tests to determine the most useful predictor variables (p-value criteria, 0.05 for entry and 0.1 for staying). These two tests allowed us to determine if the addition of automatically disqualified variables to smaller models would result in a statistically significant contribution to the final model. Potential clinical and imaging predictor variables compiled by the first author (--) were baseline serum prostatic specific antigen level, biopsy Gleason score, percentage of positive biopsies (number of positive cores divided by total number of cores), percentage of positive tissue length (millimeters of positive tissue divided by total millimeters of tissue), clinical stage, reader detection of a dominant tumor focus at MRI, tumor volume at MRI (estimated using the formula for tumor volume of $(4/3)\pi\ (D/2)^3$, where D is the average of the maximum and minimum axial diameters of the tumor at MRI), and volume of concordant spectroscopic abnormality. The assumption that the continuous fixed component predictors must have a linear correlation with the logit of the outcome was checked with the use of locally weighted scatterplot smoothing (LOWESS). The overall accuracy of the model was described using receiver operating characteristic curve analysis. We used bias corrected cluster re-sampled bootstrapping to construct 95% confidence intervals. An alpha of 5% was used for statistical significance. Statistical calculations were performed using Stata Statistical Software version 11 (StataCorp LP, College Station, TX).

Results

Histopathological findings

In the final study population (n = 88), a total of 300 prostate cancer foci were detected at histopathological review of the radical prostatectomy specimens (mean of 3.4 nodules per patient). The mean histopathological tumor volume of the dominant lesion was 3.1 cm^3 and the median dominant tumor volume was 0.023 cm^3 (range 0.004 to 33.5 cm^3). The distribution of prostate cancer foci by size is shown in Figure 1. Sixty-nine prostate cancer foci greater than 0.5 cm^3 were detected in 57 patients. Forty-six patients had a single tumor focus greater than 0.5 cm^3, 10 patients had two foci greater than 0.5 cm^3, and one patient had three foci greater than 0.5 cm^3. The sizes and Gleason scores of all tumor foci greater

than 0.5 cm^3 in the 11 patients with multiple nodules greater than 0.5 cm^3 are shown in Table 1.

Imaging findings

Readers 1 and 2 identified a dominant tumor focus on MR imaging in 50 (57%) and 58 (66%) of 88 patients, respectively. Histopathological correlation showed that 42 of the 50 (84%) suspected dominant lesions seen by reader 1 and 48 of the 58 (83%) lesions seen by reader 2 were correctly identified as dominant lesions (Figure 2). The number of suspicious or malignant voxels on MR spectroscopic imaging was the only predictor included in the final model. The volume of concordant spectroscopic abnormality was the only factor entered into our statistical model that was predictive of correct identification of a dominant intraprostatic lesion (odds ratio = 1.75; 95% confidence interval = 1.08 to 2.82; p-value = 0.02). The area under the receiver operating characteristic curve for this model was 0.86 (95% confidence interval = 0.78 to 0.93) (Figure 3). There was moderate agreement between readers with an intra-class correlation of 0.47 (95% confidence interval of 0.05 to 0.94). In particular, identification of 0.54cm^3 or more of concordant suspicious or malignant voxels resulted in identification of the dominant treatable lesion with high certainty. Using this threshold, reader 1 and 2 identified 42 and 48 patients with dominant treatable tumor foci, respectively, with no false positives.

Discussion

Our finding that concordant MRI and MR spectroscopic imaging allows for the correct identification of dominant treatable tumor foci in patients with prostate cancer should facilitate the selection of appropriate radiological candidates for MR-guided focal therapy. Our results suggest that MRI and MR spectroscopic imaging are able to correctly and confidently identify the anatomic location over half of all dominant treatable tumor foci, given that reader 1 and 2 correctly identified 42 and 48 of the 69 tumor foci over 0.5 cm^3, respectively. It is important to note that our study does not address clinical criteria for focal therapy, because no consensus exists as to which patients are best suited for this treatment option. The goal of our study was not to determine clinical criteria for focal therapy, but rather to investigate whether any imaging findings would help to identify the dominant intraprostatic lesion. Our design only required readers to identify the single largest tumor visible on MRI and used histopathological corroboration to identify a variable (suspicious or definitely malignant voxels on MR spectroscopic imaging) that affords high confidence in dominant in tumor identification.

Our study is broadly consistent with prior similar studies. A recent series of 100 consecutive radical prostatectomy specimens confirmed that the largest tumor focus is usually the most important; although 78% (78/100) of cases demonstrated multifocal disease, only 22 of 170 additional foci were over 0.5 cm^3 in size (12.9%) and only 1 had a Gleason score over 6 (25). An estimated 51% of the patients in this series were considered suitable for focal therapy, based on whether the dominant tumor focus was organ-confined, Gleason score ≤7, with the total volume of secondary foci ≤0.5 cm^3 and Gleason score ≤6. Another series of 1,000 radical prostatectomy specimens found that the largest (index) lesion represented an average of 80% of the total tumor volume, and that 92% of cases with extracapsular extension were found to have extracapsular extension emanating from the index lesion (6). Since treatment modalities such as cryoablation or focused ultrasound can extend treatment areas beyond the prostatic capsule, focal therapy may benefit patients with extracapsular extension (26). Although Gleason grade carries prognostic significance, there is no consensus on whether patients with Gleason grade 7 tumors should be excluded from focal therapy. Patients with Gleason grade 7 tumors have been included in several focal therapy studies with encouraging short-term follow-up data (27, 28). Our study may initially appear

discordant with recent literature questioning the incremental value of MR spectroscopic imaging (29), but this likely reflects the limited spatial resolution and contribution of spectroscopic across the range of smaller and lower risk tumors typically seen in patients undergoing radical prostatectomy. Spectrosopic may still be useful in the subset of these patients with larger tumors of 0.5 cm^3 or greater.

Our study has limitations. First, its retrospective nature may lead to selection bias, as all patients within the study population underwent radical prostatectomy. Our histopathological criteria of eligibility may therefore include patients with advanced Gleason grades or tumor bulk that may be later considered unsuitable for focal therapy. Second, the subjects used to calculate the performance of the model are the same as those used to fit the model on which the classification rule is based. A better approach would have been using cross-validation; unfortunately we were not able to perform such technique due to the limited number of patients in our sample. Third, we did not investigate other MRI techniques such as diffusion weighted MR-imaging or dynamically contrast-enhanced MRI. It is likely that the addition of these sequences would yield different results, perhaps improving the detection of dominant lesions. For example, diffusion weighted MRI has been shown to significantly improve tumor volume estimation in prostate cancer (30). Fourth, despite the fact that both readers correctly identified a similar number of dominant lesions, the inter-reader agreement was only moderate. In other words, other factors or random variation may have played a role in reader interpretation. Fifth, our study design was deliberately chosen to address only identification of the largest tumor focus, given that the dominant focus is usually the most important, as discussed above. That said, it is noteworthy that 11 of our 88 patients had two or more nodules of 0.5 cm^3 or greater in size, and 6 (2) of these 11 patients as evaluated by reader 1 (2) would have been considered eligible for focal therapy of the dominant lesion based on reader MR identification of the dominant lesion (Table 1). Overall, it could be argued that 6 of 42 patients identified as eligible for focal therapy by reader 1 would have been inappropriately treated, with the corresponding values for reader 2 being 2 of 48. That is, therapy would have been directed to the largest tumor focus of 0.5 cm^3 or greater in size in these patients with additional tumor foci of 0.5 cm^3 or greater in size going untreated. Further studies will be required to address the clinical or radiological features that allow for accurate identification of patients with multiple foci of treatable disease, so that these patients can be offered multifocal or standard definitive therapy. Sixth, this study did not address the admixture of benign tissue interspersed with cancer (31), a described finding that might confound the identification of tumor margins for ablation. We are currently conducting a separate study to investigate appropriate margins for MR-guided focal therapy of prostate cancer. Seventh, we calculated both MRI and histopathological tumor volumes from bidemensional axial diameters. This methodology assumes the craniocaudad diameter is the mean of the two axial diameters. It is possible that this geometric assumption is incorrect for tumors elongated in the coronal direction, but accurate histopathological measurements of the craniocudad dimension are difficult to obtain since slice intervals may be imprecise and because of errors introduced by fixation. Finally, our study is preliminary and only addresses patient selection for MR guided focal therapy, such as high intensity focused ultrasound or laser ablation. Ultimately, these emerging technologies will need more extensive validation, including demonstration of adequate cancer control and acceptable morbidity.

In conclusion, patients with dominant intraprostatic tumor foci seen on T2-weighted MRI and associated with at least 0.54 cm^3 of concordant MR spectroscopic imaging abnormality may be radiological candidates for MR guided focal therapy.

Acknowledgments

Work supported by NIH/NCRR/OD UCSF-CTSI Grant Number KL2 RR024130 and NIH Grant Number 1S10RR028911-01. Its contents are solely the responsibility of the authors and do not necessarily represent the official views of the NIH.

References

1. Onik G, Narayan P, Vaughan D, Dineen M, Brunelle R. Focal “nerve-sparing” cryosurgery for treatment of primary prostate cancer: a new approach to preserving potency. Urology. 2002; 60:109–114. [PubMed: 12100934]
2. Eggener SE, Scardino PT, Carroll PR, et al. Focal therapy for localized prostate cancer: a critical appraisal of rationale and modalities. J Urol. 2007; 178:2260–2267. [PubMed: 17936815]
3. Jayram G, Eggener SE. Patient selection for focal therapy of localized prostate cancer. Curr Opin Urol. 2009; 19:268–273. [PubMed: 19342957]
4. Polascik TJ, Mouraviev V. Focal therapy for prostate cancer is a reasonable treatment option in properly selected patients. Urology. 2009; 74:726–730. [PubMed: 19660791]
5. Ahmed HU, Emberton M. Active surveillance and radical therapy in prostate cancer: can focal therapy offer the middle way? World J Urol. 2008; 26:457–467. [PubMed: 18704441]
6. Mouraviev V, Mayes JM, Polascik TJ. Pathologic basis of focal therapy for early-stage prostate cancer. Nat Rev Urol. 2009; 6:205–215. [PubMed: 19352395]
7. Tsakiris P, Thuroff S, de la Rosette J, Chaussy C. Transrectal high-intensity focused ultrasound devices: a critical appraisal of the available evidence. J Endourol. 2008; 22:221–229. [PubMed: 18211209]
8. Han KR, Cohen JK, Miller RJ, et al. Treatment of organ confined prostate cancer with third generation cryosurgery: preliminary multicenter experience. J Urol. 2003; 170:1126–1130. [PubMed: 14501706]
9. Pauly KB, Diederich CJ, Rieke V, et al. Magnetic resonance-guided high-intensity ultrasound ablation of the prostate. Top Magn Reson Imaging. 2006; 17:195–207. [PubMed: 17414077]
10. Raz O, Haider MA, Davidson SRH, Lindner U, Hlasny E, Weersink R, Gertner MR, Kucharcyzk W, McCluskey SA, Trachtenberg J. Real time Magnetic Resonance Imaging-guided focal laser therapy in patients with low risk prostate cancer. Eur Urol. 2010; 58:173–777. [PubMed: 20334965]
11. Falzarano SM, Zhou M, Hernandez AV, Moussa AS, Jones JS, Magi-Galluzzi C. Can Saturation Biopsy Predict Prostate Cancer Localization in Radical Prostatectomy Specimens: A Correlative Study and Implications for Focal Therapy. Urology. 2010; 76:682–687. [PubMed: 20206973]
12. Scheidler J, Hricak H, Vigneron DB, et al. Prostate cancer: localization with three-dimensional proton MR spectroscopic imaging--clinicopathologic study. Radiology. 1999; 213:473–480. [PubMed: 10551229]
13. Yu KK, Scheidler J, Hricak H, et al. Prostate cancer: prediction of extracapsular extension with endorectal MR imaging and three-dimensional proton MR spectroscopic imaging. Radiology. 1999; 213:481–488. [PubMed: 10551230]
14. Coakley FV, Kurhanewicz J, Lu Y, et al. Prostate cancer tumor volume: measurement with endorectal MR and MR spectroscopic imaging. Radiology. 2002; 223:91–97. [PubMed: 11930052]
15. Hom JJ, Coakley FV, Simko JP, Qayyum A, Lu Y, Schmitt L, Carroll PR, Kurhanewicz J. Prostate cancer: Endorectal MR imaging and MR spectroscopic imaging - Distinction of true-positive results from chance-detected lesions. Radiology. 2006; 238:192–199. [PubMed: 16373767]
16. Hom JJ, Coakley FV, Simko JP, Lu Y, Qayyum A, Westphalen A, Schmitt L, Carroll PR, Kurhanewicz J. High-grade prostatic intraepithelial neoplasia in patients with prostate cancer: MR and MR spectroscopic imaging features – Initial experience. Radiology. 2007; 242:483–489. [PubMed: 17179396]
17. Westphalen AC, Coakley FV, Qayyum A, Swanson M, Simko JP, Lu Y, Zhao S, Carroll PR, Yeh BM, Kurhanewicz J. Peripheral zone prostate cancer: Accuracy of different interpretative

approaches with MR and MR spectroscopic imaging. Radiology. 2008; 246:177–84. [PubMed: 18024434]

18. Schricker AA, Pauly JM, Kurhanewicz J, Swanson MG, Vigneron DB. Dualband spectral-spatial RF pulses for prostate MR spectroscopic imaging. Magn Reson Med. 2001; 46:1079–1087. [PubMed: 11746572]
19. Star-Lack J, Vigneron DB, Pauly J, Kurhanewicz J, Nelson SJ. Improved solvent suppression and increased spatial excitation bandwidths for three-dimensional PRESS CSI using phase-compensating spectral/spatial spin-echo pulses. J Magn Reson Imaging. 1997; 7:745–757. [PubMed: 9243397]
20. Tran TK, Vigneron DB, Sailasuta N, et al. Very selective suppression pulses for clinical MRSI studies of brain and prostate cancer. Magn Reson Med. 2000; 43:23–33. [PubMed: 10642728]
21. Jung JA, Coakley FV, Vigneron DB, et al. Prostate depiction at endorectal MR spectroscopic imaging: investigation of a standardized evaluation system. Radiology. 2004; 233:701–708. [PubMed: 15564406]
22. Taouli B, Goh JS, Lu Y, et al. Growth rate of hepatocellular carcinoma: evaluation with serial computed tomography or magnetic resonance imaging. J Comput Assist Tomogr. 2005; 29:425–429. [PubMed: 16012295]
23. Polascik TJ, Mayes JM, Mouraviev V. Nerve-sparing focal cryoablation of prostate cancer. Curr Opin Urol. 2009; 19:182–187. [PubMed: 19188772]
24. Stamey TA, Freiha FS, McNeal JE, Redwine EA, Whittemore AS, Schmid HP. Localized prostate cancer. Relationship of tumor volume to clinical significance for treatment of prostate cancer. Cancer. 1993; 71:933–938. [PubMed: 7679045]
25. Karavitakis M, Winkler M, Abel P, Livni N, Beckley I, Ahmed HU. Histological characteristics of the index lesion in whole-mount radical prostatectomy specimens: implications for focal therapy. Prostate Cancer Prostatic Dis. May 25.2010 (Epub ahead of print).
26. Polascik TJ, Mayes JM, Schroeck FR, et al. Patient selection for hemiablative focal therapy of prostate cancer: variables predictive of tumor unilaterality based upon radical prostatectomy. Cancer. 2009; 115:2104–2110. [PubMed: 19288576]
27. Lambert EH, Bolte K, Masson P, Katz AE. Focal cryosurgery: encouraging health outcomes for unifocal prostate cancer. Urology. 2007; 69:1117–1120. [PubMed: 17572198]
28. Onik G, Vaughan D, Lotenfoe R, Dineen M, Brady J. The “male lumpectomy”: focal therapy for prostate cancer using cryoablation results in 48 patients with at least 2-year follow-up. Urol Oncol. 2008; 26:500–505. [PubMed: 18774463]
29. Weinreb JC, Blume JD, Coakley FV, Wheeler TM, Cormack JB, Sotto CK, Cho H, Kawashima A, Tempany-Afdhal CM, Macura KJ, Rosen M, Gerst SR, Kurhanewicz J. Prostate cancer: sextant localization at MR imaging and MR spectroscopic imaging before prostatectomy--results of ACRIN prospective multi-institutional clinicopathologic study. Radiology. 2009; 251:122–33. [PubMed: 19332850]
30. Mazaheri Y, Hricak H, Fine SW, Akin O, Shukla-Dave A, Ishill NM, Moskowitz CS, Grater JE, Reuter VE, Zakian KL, Touijer KA, Koutcher JA. Prostate tumor volume measurement with combined T2-weighted imaging and diffusion-weighted MR: correlation with pathologic tumor volume. Radiology. 2009; 252:449–457. [PubMed: 19703883]
31. Langer DL, van der Kwast TH, Evans AJ, Sun L, Yaffe MJ, Trachtenberg J, Haider MA. Intermixed normal tissue within prostate cancer: effect on MR imaging measurements of apparent diffusion coefficient and T2--sparse versus dense cancers. Radiology. 2008; 249:900–8. [PubMed: 19011187]

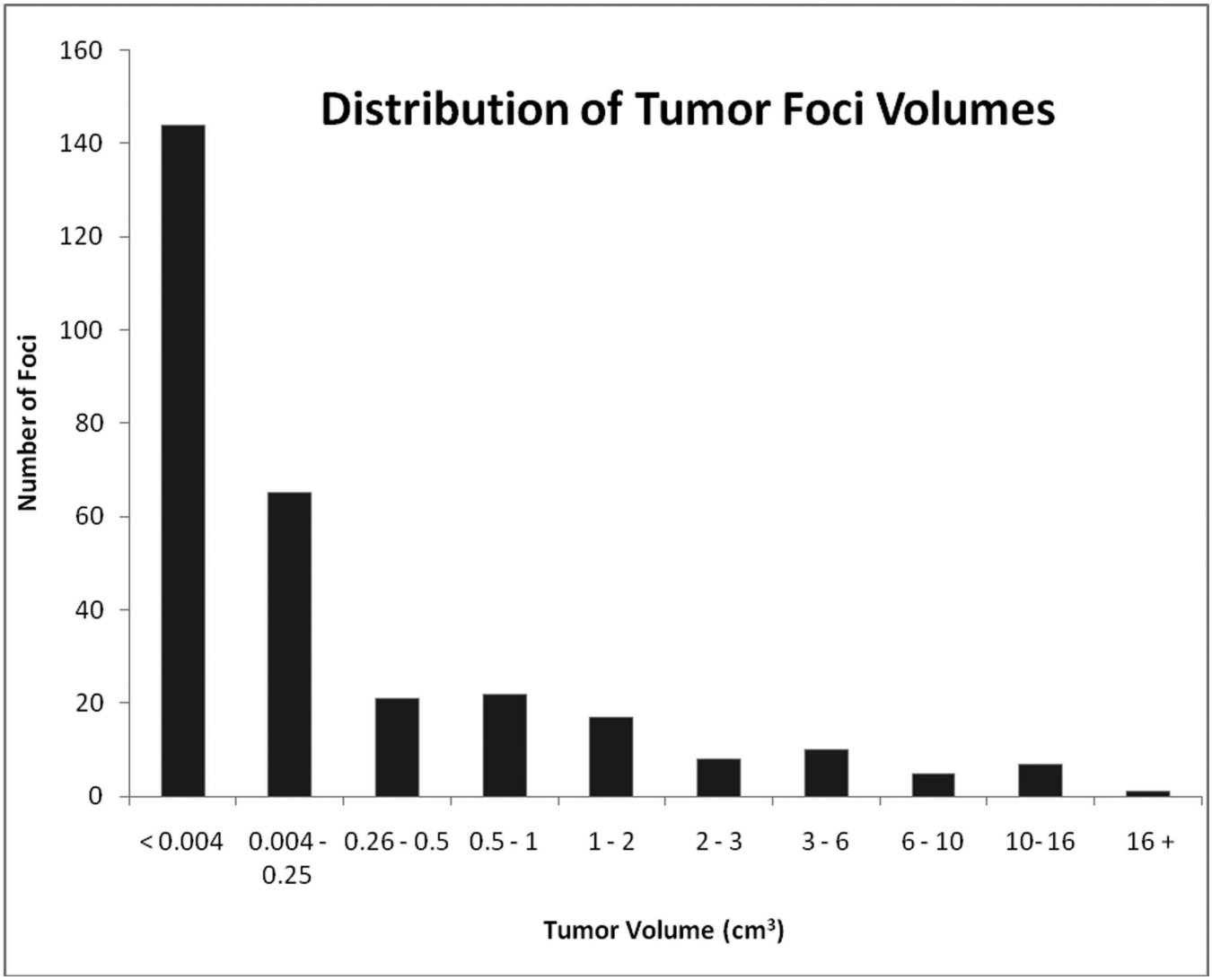

Figure 1.
Distribution by size of prostate cancer foci (n = 300 foci) detected at histopathological review of radical prostatectomy specimens (n = 88 cases).

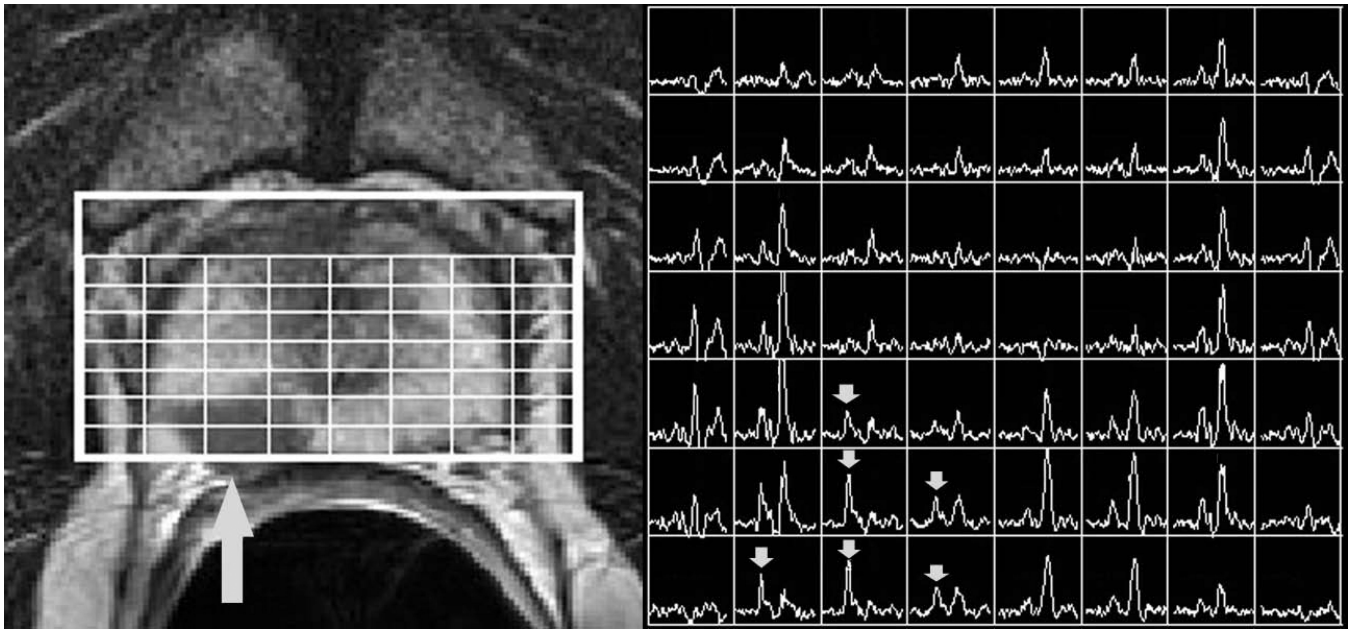

Figure 2A.
Photomontage showing an axial T2-weighted image with an overlaid grid (left side of montage) and the spectral array corresponding to the overlaid grid (right side of montage) in a 68-year-old man with a PSA of 8.2 and Gleason 7 prostate cancer on transrectal ultrasound guided biopsy. A focus of low T2 signal intensity (large arrow on left) corresponds to a cluster of voxels with elevated choline peaks (small arrows on right) and is consistent with tumor.

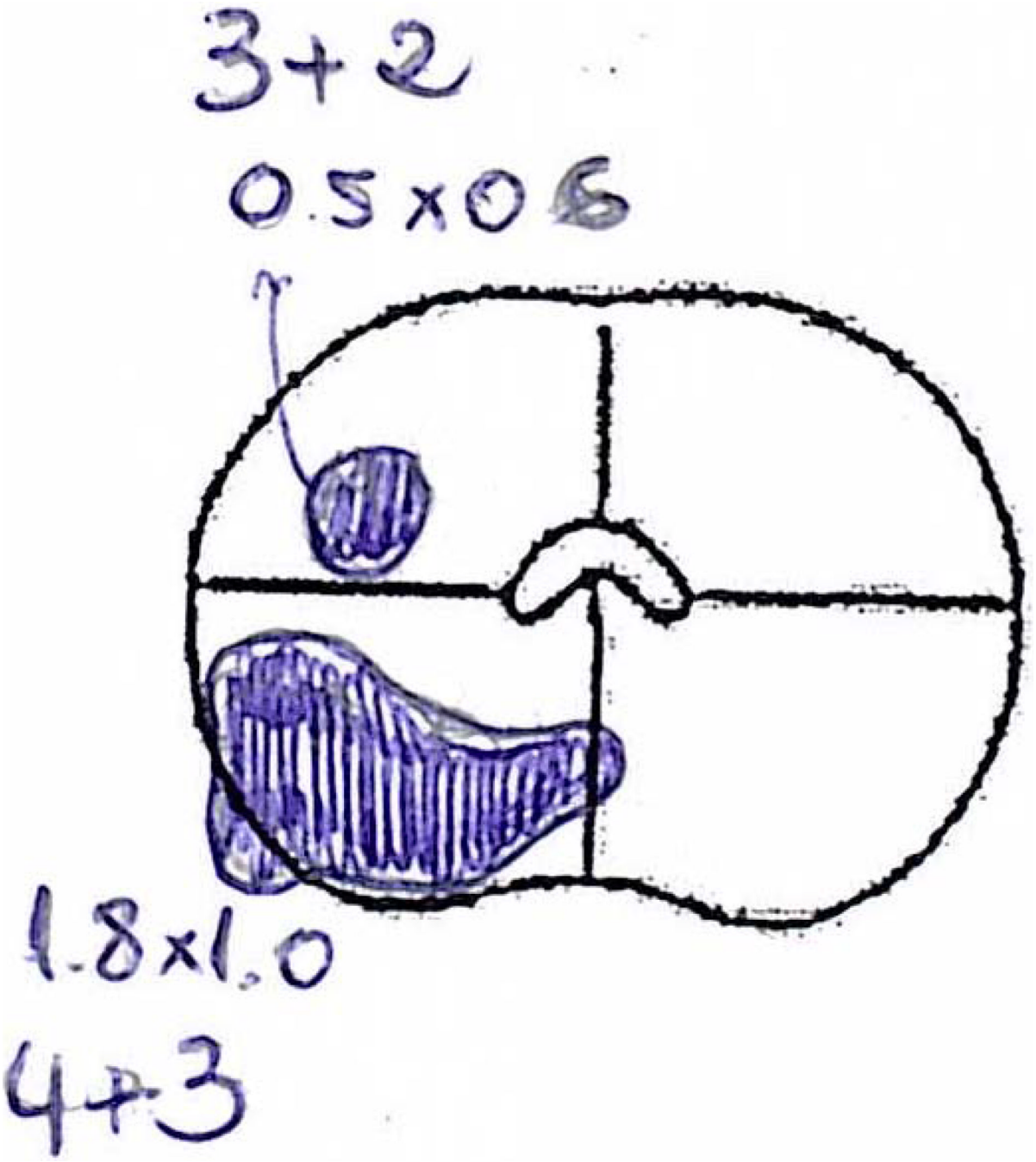

Figure 2B.

Corresponding section from a histopathological tumor map prepared after step-section review of the radical retropubic prostatectomy specimen from the patient featured in Figure 1A shows a focus of tumor in the right mid-gland that corresponds to the abnormality seen in Figure 1A (a second smaller tumor focus anteriorly is not visible on MR imaging). Handwritten annotations refer to tumor size (cm) and Gleason score. The posterior tumor was associated with extracapsular extension, as indicated by tumor extending beyond the margin of the prostate.

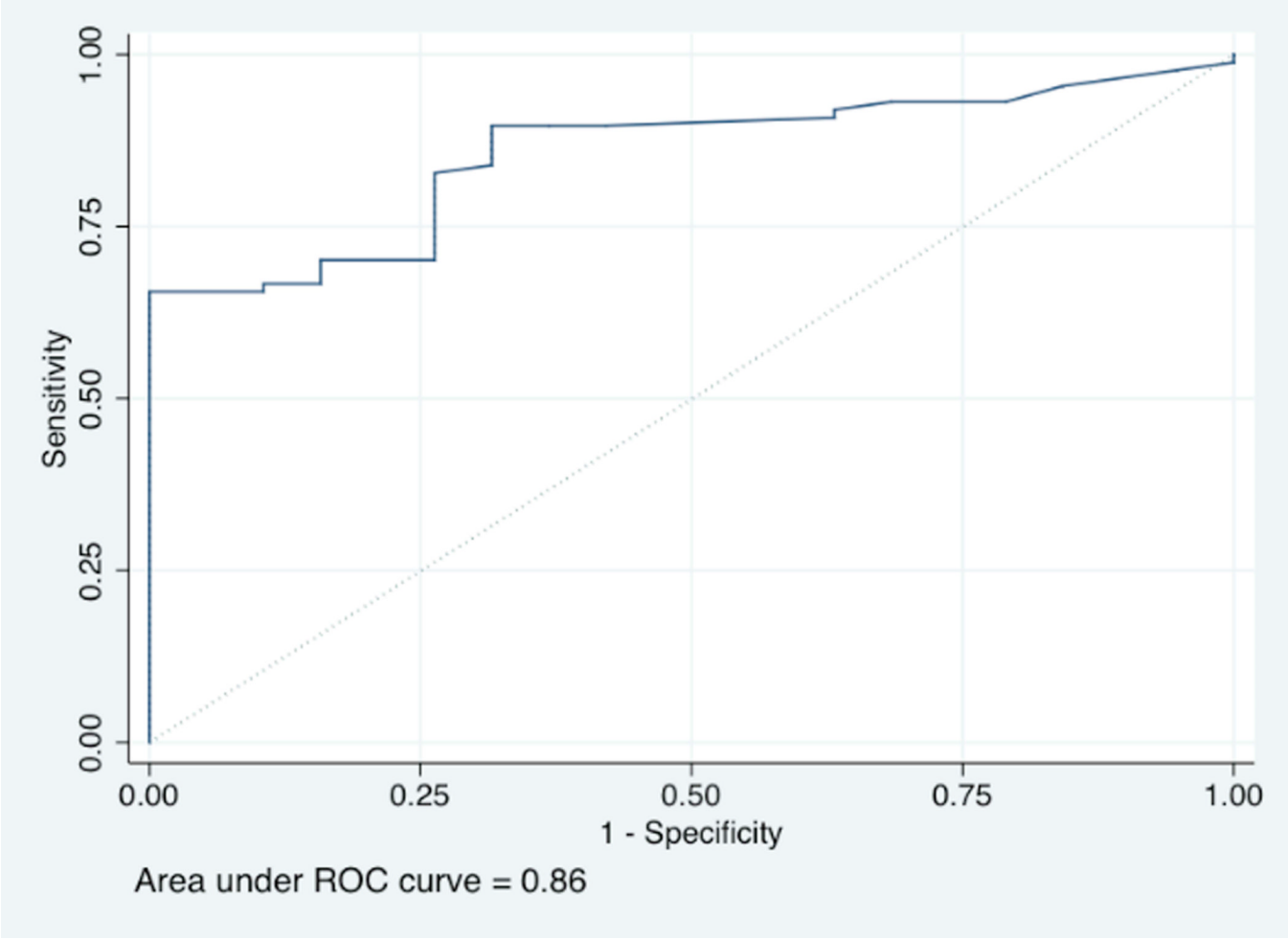

Figure 3.
The area under ROC curve was 0.86 (95% CI = 0.77 to 0.92), suggesting a good performance of the model. At a threshold of 0.54cm^3 of spectroscopic abnormality, the model has a sensitivity of 59.8% and specificity of 100%, correctly classifying 67% of cases.

Table 1

Volumes and Gleason scores of the dominant, secondary, and tertiary tumor foci in the 11 of 88 patients who had multiple tumor foci with volumes greater than 0.5 cm^3.

#t	Volume of Dominant Lesion (cm^3)	Gleason Score of Dominant Lesion	Dominant lesion treatable* (Reader 1)	Dominant lesion treatable* (Reader 2)	Volume of Secondary Lesion(cm^3)	Gleason Score of Secondary Lesion	Volume of Tertiary Lesion (cm^3)	Gleason Score of Tertiary Lesion
1	14.1	6	No	No	3.6	6		
2	12.8	9	Yes	No	0.7	6		
3	7.7	7	No	No	2.1	6		
4	5.9	8	Yes	Yes	4.5	6		
5	4.5	7	Yes	No	1.9	7		
6	4.2	7	Yes	Yes	0.5	6		
7	2.6	7	Yes	No	2.4	6	0.5	6
8	1.8	7	No	No	1.3	9		
9	1.4	7	Yes	No	0.9	5		
10	0.7	6	No	No	0.5	7		
11	0.7	7	No	No	0.5	6		

*Correctly identified and associated volume of abnormal MR spectroscopic imaging abnormality > 0.54 cm^3.